

Experimental infection of cattle with *Mycobacterium tuberculosis* isolates shows the attenuation of the human tubercle bacillus for cattle

Bernardo Villarreal-Ramos¹, Stefan Berg¹, Adam Whelan^{1,*}, Sebastien Holbert^{2,3}, Florence Carreras^{2,3}, Francisco J. Salguero⁴, Bhagwati L. Khatri¹, Kerri M. Malone⁵, Kevin Rue-Albrecht^{5,6,8}, Ronan Shaughnessy⁵, Alicia Smyth⁵, Gobena Ameni⁷, Abraham Aseffa⁸, Pierre Sarradin⁹, Nathalie Winter^{2,3}, Martin Vordermeier¹, Stephen V. Gordon^{5,10,11,12,¶}

¹Animal and Plant Health Agency, Weybridge, Surrey KT15 3NB, UK.

²Infectiologie et Santé Publique (ISP-311), INRA Centre Val de Loire, F-37380 Nouzilly, France

³Université de Tours, UMR 1282, Tours, 37000, France

⁴Department of Pathology and Infectious Diseases, School of Veterinary Medicine, University of Surrey, Guildford, UK

⁵UCD School of Veterinary Medicine, University College Dublin, Ireland.

⁶UCD School of Agriculture and Food Science, University College Dublin, Ireland.

⁷Aklilu Lemma Institute of Pathobiology, Addis Ababa University, PO Box 1176, Addis Ababa, Ethiopia.

⁸Armauer Hansen Research Institute, P O Box 1005, Addis Ababa, Ethiopia.

⁹Plate-Forme d'Infectiologie Expérimentale, PFIE, INRA, 37380, Nouzilly, France

¹⁰UCD School of Medicine, University College Dublin, Ireland.

¹¹UCD School of Biomolecular and Biomedical Sciences, University College Dublin, Ireland.

¹²UCD Conway Institute of Biomolecular and Biomedical Science, University College Dublin, Ireland.

Current Addresses:

*Biomedical Sciences, Defence Science and Technology Laboratory, Salisbury, Wiltshire SP4 0JQ, UK.

§Kennedy Institute of Rheumatology, University of Oxford, Oxford OX3 7FY, UK.

¶Corresponding author: stephen.gordon@ucd.ie

1 **Abstract**

2

3 The *Mycobacterium tuberculosis* complex (MTBC) is the collective term given to the
4 group of bacteria that cause tuberculosis (TB) in mammals. It has been reported that
5 *M. tuberculosis* H37Rv, a standard reference MTBC strain, is attenuated in cattle compared to
6 *Mycobacterium bovis*. However, as *M. tuberculosis* H37Rv was isolated in the early 1930s,
7 and genetic variants are known to exist, we sought to revisit this question of attenuation of
8 *M. tuberculosis* for cattle by performing a bovine experimental infection with a recent
9 *M. tuberculosis* isolate. Here we report infection of cattle using *M. bovis* AF2122/97,
10 *M. tuberculosis* H37Rv, and *M. tuberculosis* BTB1558, the latter isolated in 2008 during a TB
11 surveillance project in Ethiopian cattle. We show that both *M. tuberculosis* strains caused
12 reduced gross and histopathology in cattle compared to *M. bovis*. Using *M. tuberculosis*
13 H37Rv and *M. bovis* AF2122/97 as the extremes in terms of infection outcome, we used
14 RNA-Seq analysis to explore differences in the peripheral response to infection as a route to
15 identify biomarkers of progressive disease in contrast to a more quiescent, latent infection.
16 Our work shows the attenuation of *M. tuberculosis* strains for cattle, and emphasizes the
17 potential of the bovine model as a ‘One Health’ approach to inform human TB biomarker
18 development and post-exposure vaccine development.

19 **Introduction**

20

21 The *Mycobacterium tuberculosis* complex (MTBC), the group of pathogens that
22 cause tuberculosis (TB) in mammals, show distinct host preference. *Mycobacterium*
23 *tuberculosis* is the hallmark member of the MTBC and the most deadly human pathogen
24 globally, with close to 2 billion people infected worldwide¹. The animal-adapted members of
25 the MTBC are named after the host of initial/most frequent isolation, and comprise: the
26 exemplar animal pathogen and predominant agent of bovine TB *M. bovis*²; *M. microti*³; the
27 ‘Dassie bacillus’^{4,5}; *M. caprae*⁶; *M. pinnipedii*⁷; *M. orygis*⁸, and *M. mungi*⁹. A caveat is that
28 these species designations do not define host exclusivity; MTBC members can infect a range
29 of mammals to greater or lesser degrees. The central feature of host adaptation is the ability to
30 sustain within a host population. Thus, *M. bovis* can infect and cause disease in humans;
31 however, the capacity of *M. bovis* to transmit between immunologically competent humans is
32 severely limited compared to *M. tuberculosis*^{10,11}. Similarly, reports suggest that
33 *M. tuberculosis* appears attenuated in a bovine host compared to *M. bovis*¹²⁻¹⁴.

34

35 The advent of systems for mutagenesis of mycobacteria allied with (largely) murine
36 screens for phenotype has provided enormous insight into the virulence genes and pathogenic
37 strategies of mycobacteria. Yet the basis for host preference across the MTBC is largely
38 unknown. Members of the MTBC share >99% nucleotide identity across their genomes, with
39 for example ~2,400 SNPs between *M. bovis* AF2122/97 and *M. tuberculosis* H37Rv¹⁵⁻¹⁷.
40 Regions of difference (RD), deleted loci absent from one MTBC member relative to another,
41 serve as unique markers to differentiate species with some having had functional roles
42 ascribed. The RD1 locus of *M. tuberculosis* encodes a type VII secretion system whose role in
43 virulence of *M. tuberculosis* has been convincingly explored using a range of *in vitro* and
44 model systems¹⁸. However, RD1-like deletions from *M. microti* and the ‘dassie’ bacillus
45 indicate that discrete evolutionary scenarios have moulded the virulence strategies and
46 genomes of the MTBC bacilli^{19,20}. Similarly, functional impacts of single nucleotide
47 polymorphisms (SNPs) between the various MTBC and their potential role in host-pathogen
48 interaction have been described²¹. Much work remains in describing the precise host and
49 pathogen molecular factors involved in host preference²².

50

51 An essential step to defining host tropic factors is defining tractable experimental
52 models; given the range of wild and domesticated mammals that are susceptible to infection
53 by MTBC members, this is no small task. Nevertheless, with the aim of exploring MTBC host
54 preference, we have previously explored the comparative virulence of *M. tuberculosis* and
55 *M. bovis* in a bovine experimental infection model, and showed that *M. tuberculosis* H37Rv

56 was attenuated compared to *M. bovis* AF2122/97¹³. However, while *M. tuberculosis* H37Rv
57 is the reference strain of the MTBC, its isolation was first reported 1935²³ and it has been
58 maintained in multiple laboratories globally, with separate extant ‘versions’ of
59 *M. tuberculosis* H37Rv²⁴. The possibility remained that other *M. tuberculosis* clinical isolates
60 would show a different phenotype in a bovine infection. Indeed, there have been increasing
61 numbers of reports of the isolation of *M. tuberculosis* from cattle²⁵⁻²⁷, including our own
62 work where we previously isolated *M. tuberculosis* strains from lesions identified in cattle at
63 slaughter in Ethiopian cattle^{28,29}. This would suggest that either there exist strains of
64 *M. tuberculosis* with virulence characteristics that allow them to infect and cause disease in
65 cattle, or that the cattle from which these *M. tuberculosis* strains were isolated had greater
66 susceptibility to infection due to being immune comprised, co-infections, age, malnutrition, or
67 other predisposing factors such as being in an environment of continuous exposure to
68 *M. tuberculosis*.

69

70 We therefore set out to evaluate the attenuated virulence of *M. tuberculosis* in the
71 bovine host using a recent *M. tuberculosis* bovine isolate as the comparator. We chose to use
72 an Ethiopian *M. tuberculosis* strain that had been isolated from a Zebu bull, *M. tuberculosis*
73 BTB1558, to perform this new experimental infection in cattle, and to compare the virulence
74 of this latter isolate to the *M. tuberculosis* H37Rv and *M. bovis* AF2122/97 strains.

75

76 **Material and Methods**

77

78 *Ethical permission*

79 Ethical permission was obtained from the APHA Animal Use Ethics Committee (UK
80 Home Office PCD number 70/6905), AHRI/ALERT Ethics Review Committee (Ethiopia)
81 and the French Research and Education Ministry, via the Val de Loire Ethical Committee
82 (CEEAVDL, #19) for INRA (France).

83

84 *Mycobacterial strains and culturing protocols*

85 Three strains were used for this bovine challenge experiment: *M. bovis* AF2122/97 is
86 a field strain isolated from a cow in Great Britain in 1997¹⁶. *M. tuberculosis* H37Rv was from
87 the APHA culture stocks. The virulence of both the *M. bovis* AF2122/97 and *M. tuberculosis*
88 H37Rv stocks has been confirmed via inoculation of guinea pigs¹³, with both seed stocks
89 clearly virulent in this model. *M. tuberculosis* BTB1558 was isolated in 2008 from the cranial
90 mediastinal lymph node of a Zebu bull (*Bos indicus*) at Ghimbi abattoir, Ethiopia. The lesion
91 from which the strain was isolated was classed as localised, and was not caseous or calcified;
92 no nasal secretions were present at the ante-mortem investigation. An *M. tuberculosis* strain
93 of the same spoligotype as BTB1558 (SIT 764) was isolated from a human pulmonary TB
94 patient in Ethiopia³⁰; both the cattle and the human isolate have been confirmed as members
95 of the Euro-American lineage, also known as Lineage 4^{31,32}.

96

97 *M. bovis* AF2122/97 and *M. tuberculosis* BTB1558 had been passaged a maximum of
98 five times prior to the challenge experiment. Seed stocks had been cultured to mid-log phase
99 in Middlebrook 7H9 media (Difco, UK) supplemented with 10% (v/v) Middlebrook acid-
100 albumin-dextrose-catalase enrichment (Difco), 4.16 g/l sodium pyruvate (Sigma-Aldrich, UK)
101 and 0.05% (v/v) Tween 80 (Sigma-Aldrich) and stocks stored frozen at -80°C. The colony
102 forming units (CFU)/ml of bacterial stocks, infection inoculum, and homogenised tissue was
103 determined by bacterial enumeration of a serial dilution cultured on modified Middlebrook
104 7H11 agar³³. Inoculated plates were incubated at 37°C for four weeks (six weeks for tissue
105 samples) prior to enumeration of individual colonies on the agar plates. All seed stocks were
106 confirmed with a viability of approximately 2 x 10⁷ CFU/ml prior to further use.

107

108 *Preparation of *M. bovis* and *M. tuberculosis* infection inoculum*

109 Frozen seed stocks were thawed and diluted in 7H9 medium to a final concentration
110 of approximately 5 x 10³ CFU/ml. For each animal, 2ml of this infection inoculum were
111 drawn into a 5ml Luer-lock syringe. An aliquot of the *M. bovis* AF2122/97, *M. tuberculosis*
112 H37Rv, and *M. tuberculosis* BTB1558 inocula was retained to determine, retrospectively, the

113 concentration of bacilli used in each inoculum. Heat-inactivated samples of each strain were
114 used to identify the strains by large sequence polymorphism ^{29,34} and spoligotyping ³⁵.
115

116 *Cattle infection*

117 Twelve female Limousin x Simmental cattle of approximately six months of age
118 raised from birth within INRA's animal facility were divided into three groups of four. An
119 infective dose of 1×10^4 CFU was targeted for each strain; inocula were delivered
120 endobronchially in 2 ml of 7H9 medium as described previously ³⁶. In brief, animals were
121 sedated with xylazine (Rompun® 2%, Bayer, France) according to the manufacturer's
122 instructions (0.2 mL/100 kg, IV route) prior to the insertion of an endoscope through the nasal
123 cavity into the trachea for delivery of the inoculum through a 1.8 mm internal diameter
124 cannula (Veterinary Endoscopy Services, U.K.) above the bronchial opening to the cardiac
125 lobe and the main bifurcation between left and right lobes. Two ml of PBS were used to rinse
126 any remains of the inoculum into the trachea and then cannula and endoscope were
127 withdrawn. The canal through which the cannula was inserted into the endoscope was rinsed
128 with 20 ml of PBS and the outside of the endoscope was wiped with sterilizing wipes
129 (Medichem International, U.K.) prior to infection of the next animal. Retrospective counting
130 of the inocula revealed infection with 1.66×10^4 CFU *M. tuberculosis* H37Rv; 2.2×10^4 CFU
131 *M. tuberculosis* BTB1558; and 1.12×10^4 CFU *M. bovis* AF2122/97.
132

133 *Monitoring of infection by the IFN- γ release Assay (IGRA)*

134 Blood was collected from animals one day prior to the infectious challenge (-1) and
135 every two weeks after infection until the animals were culled. Heparinized whole blood
136 (250 μ l) was incubated with a selection of mycobacterial antigens: PPD-Avium (PPD-A) or
137 PPD-Bovine (PPD-B) (Prionics) respectively at 25 IU and 30 IU final; or peptide pools
138 covering ESAT6/CFP10, Rv3873 or Rv3879c added in a volume of 25 μ l to a final
139 concentration of 10 μ g/ml. Pokeweed mitogen was used as the positive control at 10 μ g/ml,
140 and a media-only negative control also included. After 24h in 5% (v/v) CO₂ atmosphere at
141 37°C stimulated bloods were centrifuged (400xg for 5 min); 120 μ l of supernatant was
142 removed and stored at -80°C for subsequent IFN- γ quantification using the Bovigam kit
143 (Prionics) in accordance with the manufacturer's instructions.

144 For RNA extractions, 4 ml of heparinized whole blood was incubated with PBS or
145 PPD-B in the same condition as described above. After 24 hr 3ml of stimulated blood were
146 transferred to Tempus™ Blood RNA tubes (Life Technologies) and stored at -80°C. The
147 remaining 1ml was centrifuged and the supernatant stored at -80°C for cytokine analyses.
148

149 *Multiplex ELISA analyses*

150 PPD-B stimulated whole blood supernatants were assayed for cytokine levels using a
151 custom-designed bovine Meso Scale Discovery® (MSD) multiplex protein analysis platform
152 (Meso Scale Discovery®, Gaithersburg, MD, USA). The bovine cytokines analysed were: IL-
153 1 β , IL-6, IL-10, IL-12, and TNF- α . Multiplex 96 well plates (supplied with target capture
154 antibodies spotted onto separate carbon electrodes in each well) were blocked with MSD®
155 assay buffer for 30 min at room temperature before the addition of 25 μ l samples or MSD®
156 standards (prepared according to manufacturer's instructions). Following 2h sample
157 incubation at room temperature, plates were washed and incubated for a further 2h with a
158 combined cocktail of biotinylated detection antibodies for each cytokine and MSD® SULFO-
159 TAG™-labelled Streptavidin (according to the manufacturers' instructions). After a final
160 wash, plates were coated with MSD® Buffer-T and luminescence (OD_{455nm}) was measured on
161 a SECTOR® Imager 6000 instrument (MSD). IL-6, IL-10 and IL-12 responses are reported as
162 U/ml while IL-1 β and TNF- α responses are reported in ng/ml as interpolated from the
163 standard curves for each cytokine included on each plate.

164

165 *Gross pathology and histopathology*

166 Ten weeks after infection animals inoculated with *M. tuberculosis* were killed and
167 subjected to post-mortem analysis as indicated elsewhere³⁷; animals inoculated with *M. bovis*
168 were sacrificed six weeks after infection for post-mortem analysis as above. The presence of
169 gross pathological TB-like lesions was scored as previously described (37). For histology, a
170 cross-sectional slice of the lymph node was collected into a 100 ml pot containing buffered
171 formalin. Collected tissue samples were shipped overnight from INRA to APHA Weybridge
172 for subsequent processing.

173 Tissues evaluated for gross pathology included the following lymph nodes: left and
174 right parotid, lateral retropharyngeal, medial retropharyngeal, submandibular, caudal, cranial
175 mediastinal and cranial tracheobronchial and pulmonary lymph nodes; lung tissue samples
176 were also taken. Tissue samples were preserved in 10% phosphate buffered formalin for 7
177 days before being embedded in paraffin wax. Four-micron sections were cut and stained with
178 hematoxylin and eosin (H&E); Ziehl-Neelsen staining was carried out for the detection of
179 acid-fast bacilli (AFB). For histopathology, sections of thoracic (caudal mediastinal, cranial
180 mediastinal, cranial tracheobronchial, left and right bronchial) and extrathoracic (left and right
181 parotid, left and right medial retropharyngeal, left and right lateral retropharyngeal, left and
182 right mandibular) lymph nodes, left and right tonsils and lung were stained with for
183 examination by light microscopy to assess the number, developmental stage and distribution
184 of each granuloma (I-IV) as well as assessing the quantity and location of AFB as previously
185 described^{38,39}.

186

187 *Evaluation of tissue bacterial load*

188 For bacteriology, up to 20 g of tissue was collected into 25 ml sterile containers and
189 frozen at -80°C on the day of collection. Frozen tissues were shipped at +4°C to APHA
190 Weybridge and immediately upon arrival were homogenised using a Seward Stomacher
191 Paddle Blender with bacterial enumeration undertaken as previously described³⁷. Macerates
192 were plated on modified 7H11 agar plates containing 10% (vol/vol) Middlebrook oleic acid-
193 albumin-dextrose-catalase enrichment³³. Plates were seeded with 500µl, 50µl and 5µl of
194 macerate; 450µl and 500µl of PBS was added to the plates containing 50µl and 5µl
195 respectively to help distribute the macerate on the whole plate. Using this method the limit of
196 detection was 2 CFU/ml.

197

198 *RNA extraction and library preparation*

199 Thirty-two strand-specific RNA-Seq libraries were prepared from whole blood from
200 *M. bovis* AF2122/7 and *M. tuberculosis* H37Rv infected animals (n=4) at day 14 and day 42
201 that were either stimulated or not with PPD-B. Total RNA including miRNA was extracted
202 from the Tempus™ Blood RNA Tubes using the Preserved Blood RNA Purification Kit I
203 (Norgen Biotek Corp, Canada) according to the manufacturer's instructions. Twelve random
204 samples were chosen to assess RNA integrity using the RNA 6000 Nano Kit (Agilent) in
205 conjunction with the Agilent 2100 Bioanalyzer. RNA Integrity Numbers (RINs) ranged from
206 8 to 9.1 (8.6 average). RNA was quantified using the NanoDrop™ ND-1000
207 Spectrophotometer (Thermo Fisher Scientific) and 200ng of total RNA was subjected to two
208 rounds of Poly(A) mRNA purification using the Dynabeads® mRNA DIRECT™ Micro Kit
209 (Invitrogen™) according to the manufacturer's recommendations. The samples were prepared
210 for sequencing using the ScriptSeq™ v2 RNA-Seq Library Preparation Kit, Index PCR
211 Primers and the FailSafe™ PCR enzyme system according to manufacturer's specifications
212 (Illumina® Inc., Madison, WI, USA). The Agencourt® AMPure® XP system (Beckman
213 Coulter Genomics, Danvers, MA, USA) was utilised to purify the resulting RNA-Seq
214 libraries. Libraries were quantified using the Quant-iT dsDNA Assay Kit and subsequently
215 pooled in equimolar concentrations (Thermo Fisher Scientific). The 32 sequencing libraries
216 were pooled and sequenced over three lanes of an Illumina HiSeq 2500 Rapid Run flow cell
217 (v1) in paired end (2 x 100 bp) format by Michigan State University Research Technology
218 Support Facility, Michigan, USA. Base-calling and demultiplexing was performed with
219 Illumina Real Time Analysis [v1.17.21.3] and Illumina Bcl2Fasta [v1.8.4] respectively. The
220 RNA-Seq data has been deposited in the European Nucleotide Archive, accession number
221 PRJEB22247.

222

223 *RNA-Seq pipeline*

224 The pipelines used for the analysis of the RNA-Seq data are available on GitHub
225 (<https://github.com/kerrimalone>). Computational analyses were performed on a 32-node
226 Compute Server with Linux Ubuntu [version 12.04.2]. Briefly, pooled libraries were
227 deconvoluted, adapter sequence contamination and paired-end reads of poor quality were
228 removed using cutadapt [v1.13] (Phred > 28)⁴⁰ and the filterbytile.sh script from the BBMap
229 package⁴¹. At each step, read quality was assessed with FastQC [v0.11.5]⁴². Paired-end reads
230 were aligned to the *Bos taurus* reference genome (*B. taurus* UMD 3.1.1) with the STAR
231 software⁴³. Read counts for each gene were calculated using featureCounts, set to
232 unambiguously assign uniquely aligned paired-end reads in a stranded manner to gene exon
233 annotation (*B. taurus* UMD 3.1.1 GCF_000003055.6)⁴⁴. Differential gene expression
234 analysis was performed using the edgeR Bioconductor package that was customised to filter
235 out all bovine ribosomal RNA (rRNA) genes, genes displaying expression levels below one
236 count per million (CPM) in at least four individual libraries and identify differentially
237 expressed (DE) genes correcting for multiple testing using the Benjamini-Hochberg method
238 with a log₂ fold change (log₂FC) greater than 1/less than -1 and a False-Discovery Rate (FDR)
239 threshold of significance ≤ 0.05 ⁴⁵. DE gene expression was evaluated between *M. bovis* and
240 *M. tuberculosis* infected animals for unstimulated blood samples (unpaired statistics) for each
241 time point in addition to between unstimulated and PPD-B-stimulated blood samples for the
242 *M. bovis* and *M. tuberculosis* infected animals independently at each time point (paired
243 statistics). Cellular functions and pathways over-represented in DE gene lists were assessed
244 using the SIGORA R package while graphical representation of data results was achieved
245 using the R packages ggplot2, VennDiagram and related supporting packages⁴⁶⁻⁴⁸.

246

247 *miRNA RT-qPCR*

248 MicroRNA miR-155 was selected for analysis based on its suggested role in immune
249 response to *M. bovis* infection⁴⁹. As the human and bovine sequences are identical, hsa-miR-
250 155-5p primers were purchased from Exiqon miRCURY UniRT miRNA primers (catalogue
251 number 204308).

252

253

254

255 **RESULTS**

256

257 *Immune response in infected cattle*

258 Three groups of four cattle each were infected endobronchially with 1.66×10^4 CFU
259 *M. tuberculosis* H37Rv, 2.2×10^4 CFU *M. tuberculosis* BTB1558, or 1.12×10^4 CFU *M. bovis*
260 AF2122/97, respectively. Because of the need to restrict the total time the experiment would
261 run in the containment facility, animals infected with *M. tuberculosis* strains H37Rv or
262 BTB1558 were maintained for 10 weeks, while *M. bovis* AF2122/97-infected animals were
263 maintained for 6 weeks, after which all animals underwent post-mortem examination. Antigen
264 specific IFN- γ responses were detected against both PPD-B (data not shown) and a cocktail of
265 ESAT-6/CFP-10 peptides (Figure 1) two to three weeks after infection, with no significant
266 difference in responses between groups over the course of the infections.

267 In previous work ¹³ we had seen that while stimulation of whole blood with the
268 antigen Rv3879c triggered IFN- γ production in *M. bovis*-infected cattle, *M. tuberculosis*
269 H37Rv-infected cattle showed no responses. In this current work Rv3879c stimulation of
270 whole blood provided less definitive outcomes, as while Rv3879c triggered minimal IFN- γ
271 responses in blood from *M. tuberculosis* H37Rv or BTB1558 infected animals, the baseline
272 responses to Rv3879c stimulation in *M. bovis* AF2122/97 infected cattle were high prior to
273 infection, and showed no increase in response over the course of infection (data not shown).

274 Supernatants from PPD-B stimulated samples were also checked for IL-1 β , IL-6, IL-
275 10, IL-12, and TNF- α production over the course of infection using the MSD multiplex
276 platform (Figure 2). Over the first 6 weeks after infection, all animals showed similar
277 responses to all strains, although *M. tuberculosis* BTB1558 generated higher IL-1 β responses
278 at day 28 compared to responses induced by *M. tuberculosis* H37Rv or *M. bovis* AF2122/97.
279 *M. tuberculosis* BTB1558 induced higher production of IL-10, IL-12, and TNF- α than
280 *M. tuberculosis* H37Rv at the later time points (days 56 and 70) due to responses waning in
281 the *M. tuberculosis* H37Rv group from day 42 onwards. Less than 1U/mL of IL-6 were
282 detected in both infection groups (data not shown).

283

284 *Gross pathology*

285 As described above, animals infected with *M. bovis* AF2122/97 were culled 6 weeks
286 post-infection, while *M. tuberculosis* groups were culled after 10 weeks. Lungs and lymph
287 nodes (thoracic and extrathoracic) were examined for gross lesions. Typical gross lesions
288 were isolated granulomas or coalescing clusters of granulomas of variable size ranging from 5
289 to 10 mm in diameter. Gross pathology scores are summarised in Figure 3(A-D). Statistically
290 significant differences were observed in lung gross lesions of animals infected with *M. bovis*
291 compared to animals infected with *M. tuberculosis* H37Rv or *M. tuberculosis* BTB1558; no

292 significant differences were observed comparing the lung lesions of the two sets of
293 *M. tuberculosis* infected animals. Lung gross lesions were only observed in animals infected
294 with *M. bovis* AF2122/97 with scores ranging from 5 to 10 and scores of 0 (no visible lesions)
295 in animals infected with *M. tuberculosis* H37Rv or BTB1558. Thoracic lymph nodes (cranial
296 mediastinal, caudal mediastinal, right bronchial, left bronchial and cranial tracheobronchial)
297 showed a scores of between 4 and 14 in animals infected with *M. bovis* AF2122/97; animals
298 infected with *M. tuberculosis* H37Rv had a score of 1; animals infected with *M. tuberculosis*
299 BTB1558 had scores ranging of between 0 and 2; statistically significant differences were
300 observed only between animals infected with *M. bovis* AF2122/97 and those infected with
301 *M. tuberculosis* BTB1558. Extra-thoracic lymph nodes from the head and neck region (right
302 and left lateral retropharyngeal, right and left medial retropharyngeal, right and left parotid
303 and right and left submandibular) showed scores of between 0 and 7 in animals infected with
304 *M. bovis* AF2122/97; scores of between 0 and 2 in animals infected with *M. tuberculosis*
305 BTB1558; animals infected with *M. tuberculosis* H37Rv did not show any gross visible
306 lesions in extra-thoracic lymph nodes. No statistically significant differences were observed
307 between the three groups of infected animals in the lesions observed in these nodes. No
308 lesions were found in the tonsils in any group. All animals showed TB-like gross lesions in at
309 least one organ.

310

311 *Culture of M. bovis and M. tuberculosis from processed samples.*

312 The presence of bacteria in the harvested tissue samples was investigated by semi-
313 quantitative culture (Table 1). It was possible to culture the respective infecting strain from at
314 least one organ from all experimental animals. However, the number of CFU/ml was usually
315 low for animals infected with either of the two *M. tuberculosis* strains, with zero bacterial
316 counts recorded in the lung or lung lymph nodes for all eight animals infected with either
317 strain of *M. tuberculosis*. Respiratory lymph nodes were mostly affected, with all 12 animals
318 having bacterial counts in this organ system (Table 1).

319

320 *Histopathology*

321 In H&E stained sections, four stages of granulomas were identified as previously
322 described ^{39,50}. Briefly, Stage I (initial) granulomas comprised clusters of epithelioid
323 macrophages, low numbers of neutrophils and occasional Langhans' multinucleated giant
324 cells (MNGCs). Stage II (solid) granulomas were more regular in shape and surrounded by a
325 thin and incomplete capsule. The cellular composition was primarily epithelioid
326 macrophages, with Langhans' MNGCs present and some infiltration of lymphocytes and
327 neutrophils. Necrosis was minimal or not present. Stage III (necrotic) granulomas were all
328 fully encapsulated with central areas of necrosis. The necrotic centres were surrounded by

329 epithelioid macrophages and Langhans' MNGCs, and a peripheral zone of macrophages,
330 clustered lymphocytes and isolated neutrophils extended to the fibrotic capsule. Stage IV
331 (mineralised) granulomas were completely surrounded by a thick fibrous capsule and
332 displayed central areas of caseous necrosis with extensive mineralization. The central necrosis
333 was surrounded by epithelioid macrophages and Langhans' MNGCs cells with a peripheral
334 zone of macrophages and dense clusters of lymphocytes just inside the fibrous capsule.
335 Granulomas were frequently multicentric, with several granulomas coalescing.

336 The number of granulomas of each stage in each tissue was variable (Table 2). Most
337 of the histopathological lesions were observed in the thoracic lymph nodes with only two
338 animals from BTB1558 and two others from the *M. bovis* AF2122/97 group showing
339 granulomas in extrathoracic lymph nodes. The number of granulomas observed in tissues
340 from animals infected with *M. bovis* AF2122/97 was significantly higher than the small
341 number of granulomas observed in animals infected with either strain of *M. tuberculosis*.
342 Moreover, the majority of granulomas observed in both H37Rv and BTB1558 infected
343 animals were classed as stage I, with a few stage II granulomas, while *M. bovis* AF2122/97
344 infected animals showed granulomas of all development stages (I-IV) (Table 2). AFBs were
345 identified in at least one ZN stained tissue section from every animal (data not shown)

346

347 *Transcriptome analysis of M. bovis AF2122/97 and M. tuberculosis H37Rv infected animals*

348 As the peripheral immune responses were broadly similar across all groups, yet
349 pathological examination revealed significant differences, we used transcriptomic analysis of
350 stimulated and non-stimulated whole blood samples as an unbiased tool to identifying global
351 peripheral blood markers that would correlate with the pathological outcomes. We chose to
352 analyse just the *M. bovis* AF2122/97 and *M. tuberculosis* H37Rv groups as they presented the
353 extremes in terms of immune responses and pathological presentations. Blood samples
354 cultured with medium alone (negative control) or with PPD-B from *M. bovis* AF2122/97
355 (n=4) and *M. tuberculosis* H37Rv (n=4) infection groups at days 14 and 42 were selected for
356 analysis. Strand-specific RNA-Seq libraries (n =32) were prepared from these blood samples
357 and after sequencing on an Illumina HiSeq 2500, quality-control and filtering of sequencing
358 reads yielded a mean of 14,981,780 paired-reads per individual library (2 x 100 nucleotides);
359 these data satisfy previously defined criteria for RNA-Seq experiments with respect to
360 sequencing depth ⁵¹⁻⁵³. Alignment of filtered paired-end reads to the *B. taurus* reference
361 genome UMD3.1.1 yielded a mean of ~13.5 million read pairs (~90.5%) mapping to unique
362 locations per library. Gene count summarisation resulted in an average of 59% of read pairs
363 being assigned to *B. taurus* reference genome annotations based on strict sense strand and
364 counting specifications. Gene filtering resulted in 17,663 sense genes (57.5% of all *B. taurus*
365 reference genes in the RefSeq annotations) that were suitable for differential expression

366 analysis. Multidimensional scaling analysis amongst the 32 sequencing libraries using the
367 filtered and normalised gene counts ($n = 17,663$ genes) revealed that PPD-B stimulation was
368 the largest discriminator that placed the samples into two distinct groups (Figure S1).

369

370 *Differential gene expression in unstimulated whole blood from *M. bovis* AF2122/97 and*

371 *M. tuberculosis* H37Rv infected animals

372 Pairwise analysis of the transcriptome from unstimulated bovine whole blood
373 samples at day 42 versus day 14 revealed increases in the number of differentially expressed
374 (DE) genes at day 42 post infection with either *M. bovis* AF2122/97 or *M. tuberculosis*
375 H37Rv (Figure 5A), with a greater number of genes found differentially expressed in
376 *M. tuberculosis* H37Rv infected animals at day 42, respectively (344 vs. 70 genes).

377 Direct comparison of unstimulated whole blood samples between *M. bovis*
378 AF2122/97 and *M. tuberculosis* H37Rv infected animals at day 14 and again at day 42
379 revealed 523 and 76 DE gene respectively, with 27 of these identified as DE at both time-
380 points (Figure 5A, green) between the two infection models. Amongst the top 10 DE genes
381 upregulated in *M. bovis* AF2122/97 infected animals (or conversely, downregulated in
382 *M. tuberculosis* H37Rv animals) included those encoding: the macrophage restricted cell
383 surface receptor *SIGLEC1* that is known to be involved in pathogen uptake, antigen
384 presentation and lymphocyte proliferation⁵⁴; the CD4-coreceptor and fractalkine receptor
385 *CX3CR1*, which has been linked to tuberculosis susceptibility and the impairment of
386 macrophage and dendritic cell migration^{55,56}; and Interferon-Regulated Resistance GTP-
387 Binding Protein (*MX1*) at day 14 (Figure 5B). At day 42 the expression of the following genes
388 was at relatively higher level in *M. bovis* AF2122/97 infected animals than in *M. tuberculosis*
389 H37Rv infected animals (Figure 5B): *CXCL9*, a previously described potential TB biomarker^{50,57};
390 mediator of mycobacterial-induced cytokine production in macrophages *CD180*⁵⁸; and
391 the chemokine *CXCL11*.

392 T-cell chemotactic factor *CCL17* had the highest log-fold change in *M. tuberculosis*
393 H37Rv infected samples in comparison to *M. bovis* AF2122/97 infections at day 14. Genes
394 also expressed to a higher level in *M. tuberculosis* infected animals at day 14 were: the
395 defensin *DEFB10*; platelet aggregation inducing factor *PDPN*, which is expressed on
396 macrophages and epithelioid cells within the tuberculous granuloma⁵⁹; macrophage lipid
397 export complex member *ABCG1*; and *IL6* (in contrast with the ELISA data from the same
398 time point, Figure 2). At day 42 post infection the fractalkine receptor *CX3CR1*, a marker of
399 Th1 stage differentiation during tuberculosis⁶⁰, and the V-ATPase subunit gene *ATP6V0D2*
400 were higher in *M. tuberculosis* H37Rv infected samples (Figure 5B).

401 Pathway enrichment analysis revealed pathways such as *Extracellular matrix*
402 *organization* (R-HSA-1474244), *Collagen degradation* (R-HSA-1442490), *Interferon*

403 *alpha/beta signaling* (R-HSA-909733) and B cell receptor second messenger signaling (R-
404 HSA-983695) being significantly associated with the 523 DE genes between *M. tuberculosis*
405 and *M. bovis* AF2122/97 infected animals at day 14 (Bonferroni < 0.005) (Figure 6C, 6D).
406 Further investigation revealed higher expression of 25/44 genes belonging to the antigen
407 activation of B cell receptor signaling pathway (R-HSA-983695) in *M. bovis* AF2122/97
408 infected animals at day 14, such as membrane associated *CD19*, *CD80*, *TREM2* and second
409 messengers *LYN*, *SYK*, *BTK*, *BLNK*, *PLCG2* along with B-cell receptor encoding genes
410 *CD79a* and *CD79b* (Figure 6D). The enrichment of collagen degradation and extracellular
411 matrix organization pathways in the 523 DE gene list highlighted genes of the matrix
412 metallopeptidase (MMP) family such as *MMP1*, *MMP3*, *MMP12* and *MMP14* (Figure 6C).
413 MMP proteins have been linked to leukocyte migration and the progression of granuloma
414 formation during tuberculosis; *MMP1* and *MMP14* gene products are key for the destruction
415 of collagen and alveolar destruction with an increased expression of *MMP14* gene found in
416 the sputum of tuberculosis patients^{61,62}. Gene expression of the matrix-associated cytokine
417 *SPP1* (i.e. Osteopontin/OPN) was upregulated in *M. bovis* infected animals at day 14. *SPP1*
418 enhances IFN- γ and IL-12 production, and increased levels of *SPP1* have been reported in the
419 blood of TB patients versus controls⁶³.

420 Pathway enrichment analysis with the 76 common DE genes at day 42-post infection
421 revealed no significantly associated pathways.

422

423 *Differential gene expression in PPD-B-stimulated whole blood from *M. bovis* AF2122/97 and*

424 *M. tuberculosis* H37Rv infected animals

425 To assess antigen-stimulated alteration in the whole blood transcriptome, blood
426 samples were stimulated with PPD-B overnight and subsequently compared to unstimulated
427 blood samples. PPD-B stimulation resulted in the differential expression of 2,622 and 1,586
428 genes at day 14 and 1,446 and 2,107 at day 42 in *M. bovis* AF2122/97 and *M. tuberculosis*
429 H37Rv infected animals respectively in comparison to control samples (Figure 6A).

430 Firstly, a “core” response to PPD-B stimulation amounting to 658 genes was
431 identified, representing genes that were consistently DE regardless of infectious agent or time
432 post infection (Figure 6A). As expected, *IFNY* was strongly upregulated in stimulated blood
433 samples at both time points in both *M. bovis* AF2122/97 and *M. tuberculosis* H37Rv infected
434 animals (Figure 6B). Furthermore, 47/152 genes from the *Interferon gamma signaling*
435 pathway (R-HSA-877300) were significantly differentially expressed ($-0.75 < \log_2\text{FC} > 0.75$)
436 across the comparative groups and time points (Figure 6B). Pathway enrichment analysis of
437 the 658 core response genes revealed significantly associated pathways such as those
438 involved in TNF-signaling (R-HSA-5668541, R-HSA-5676594, R-HSA-5357786, R-HSA-
439 5669034), *Chemokine receptors bind chemokines* (R-HSA-380108), *Antigen processing*-

440 *Cross presentation* (R-HSA-1236975) and *Initial triggering of complement* (R-HSA-173736)
441 (Figure 6C). The change in expression of the genes within these pathways can be seen in
442 Figure 6D; an overall downwards trend in genes encoding complement related factors was
443 found (e.g. *C1Q1*, *C1QA*, *CFD* and *CFP*) along with strong upregulation of TNF-signaling
444 related factors (e.g. *TNF*, *NFKB2*, *TNFAIP3* and lymphotoxins alpha and beta *LTA/LTB*)
445 upon PPD-B stimulation of whole blood samples (Figure 6D).

446 Second, there are 159 and 179 DE genes in either *M. bovis* AF2122/97 or
447 *M. tuberculosis* H37Rv infected animals at both time points (Figure 6A). These 338 genes
448 represent a divergence in response to PPD-B stimulation between the two infection groups
449 and the top ranking genes amongst them are presented in Figure S2 (log₂FC ratio). The
450 increased expression of *CCL17*, *DEFB10* and matrix metalloproteinase *MMP12* with the
451 decreased expression of *bactericidal permeability increasing protein BPI*, *CD164* and *IL5*
452 receptor *IL5RA* can differentiate *M. bovis* AF2122/97 infected animals from *M. tuberculosis*
453 H37Rv infected animals at both day 14 and day 42 post infection upon PPD-B stimulation.
454 Conversely, the increased expression of interferon inducible dyamin *MX2* at day 14 and
455 cytokine receptors *IL22RA2* and *XCR1* at day 42 post infection, and decreased expression of
456 T-cell regulator *TNFSF18* at day 14- and *TLR5*, defensin *DEFB5* and V-ATPase subunit gene
457 *ATP6V0D2* at day 42- post infection, distinguished *M. tuberculosis* H37Rv infected from
458 *M. bovis* AF2122/97 infected animals upon PPD-B stimulation.

459

460 *miR-155 analysis*

461 miR-155 has been identified as a potential biomarker of disease development and/or severity
462 in cattle infected with *M. bovis*⁴⁹. To explore its utility, we analysed the expression of miR-
463 155 in whole blood from *M. bovis* AF2122/97 and *M. tuberculosis* H37Rv infected cattle in
464 PPD-B stimulated vs. unstimulated whole blood over the infection time course using RT-
465 qPCR (Figure S3). The animals infected with *M. tuberculosis* H37Rv showed a steady
466 increase in expression of miR-155 after PPD-B stimulation over the course of infection, while
467 *M. bovis* infected animals showing a greater baseline expression prior to infection and hence a
468 more modest increase over the time course. While a single miRNA may lack specificity as a
469 biomarker, these results support the potential of miR-155 as a part of a biomarker panel to
470 assess infection with tubercle bacilli.

471

472

473 **Discussion**

474 This work set out to explore whether a recent isolate of *M. tuberculosis*, recovered
475 from a TB lesion identified in an Ethiopian bull, would trigger a similar immunological and
476 pathological response to the *M. tuberculosis* H37Rv reference strain when used to
477 experimentally infect cattle. This work sought to build on our previous study that had shown
478 *M. tuberculosis* H37Rv to be attenuated in the bovine host but using a recent clinical isolate to
479 address issues around possible laboratory-adaptation of the H37Rv strain that may have
480 reduced its virulence in the bovine model. Furthermore we wished to see whether the
481 application of transcriptomics would reveal potential biomarkers to differentiate between the
482 initial stages of a progressive, active *M. bovis* infection and a more quiescent, latent infection
483 with *M. tuberculosis*.

484

485 Our results showed that both *M. tuberculosis* BTB1558 and *M. tuberculosis* H37Rv
486 were considerably attenuated in the bovine host when compared to *M. bovis* AF2122/97. This
487 is despite the fact that animals infected with either *M. tuberculosis* strain were left to progress
488 for 10 weeks, while the *M. bovis* infected animals were culled 6 weeks after infection.
489 *M. bovis* induced a greater level of pathology than either of the *M. tuberculosis* strains.
490 Although *M. tuberculosis* BTB1558 appeared to induce a slightly greater level of pathology
491 in head lymph nodes than *M. tuberculosis* H37Rv, this difference was not significant; no
492 difference was detected in the level of pathology induced by either of the *M. tuberculosis*
493 strains in respiratory lymph nodes or lungs. The apparent arrest of *M. tuberculosis*
494 granulomas in stages I and II, compared to infection with *M. bovis* that produced lesions from
495 stages I-IV is another striking difference in infection outcome. The bacteriological culture
496 results showed that both strains of *M. tuberculosis* persisted in cattle, at least over the 10
497 weeks of the infection time course.

498

499 The kinetics and magnitude of peripheral blood responses across all three infection
500 groups were broadly similar over the initial 6 week phase of infection. As analysis of antigen-
501 induced peripheral blood cytokine responses failed to reflect the distinct pathological
502 presentations between the *M. bovis* AF2122/97 and *M. tuberculosis* groups, we applied RNA-
503 Seq transcriptomics of whole blood in an attempt to identify biomarkers that would better
504 distinguish the groups, focusing on the *M. bovis* AF2122/97 and *M. tuberculosis* H37Rv
505 groups. This analysis revealed discrete genes and pathways that distinguished the groups and
506 were indicative of accelerated disease development in the *M. bovis* AF2122/97 infected
507 animals, and included previously described biomarkers of disease progression or
508 susceptibility such as MMPs, CX3CR1, CXCL9 and SSP1/OPN^{50,57,60,62,63}. These changes in

509 peripheral gene expression over the course of infection provide biomarker candidates of
510 disease progression for validation in new studies.

511

512 Classic experiments from the late 19th century by Smith, Koch and von Behring
513 showed that bovine and human tubercle bacilli showed distinct virulence in animal models,
514 and in particular that the human bacillus was attenuated when used to infect cattle. Our work
515 has recapitulated these findings, using both the standard *M. tuberculosis* H37Rv strain as well
516 as an *M. tuberculosis* isolate (BTB1558) recovered from a bovine lesion. The attenuation
517 shown by the *M. tuberculosis* BTB1558 strain in this experimental model, compared to that
518 seen in the field situation in Ethiopia, therefore appears likely due to increased susceptibility
519 of the affected animal. It should be noted however that from a human and animal health
520 perspective, it is possible that cattle infected with *M. tuberculosis* may still be transmissible
521 and shed bacilli (e.g. through nasal secretions, aerosol from the lungs or through milk) albeit
522 at low levels. Such scenarios are more probable in countries where the case rates of active
523 human TB are high, interaction between humans and cattle are frequent, and consumption of
524 raw milk common.

525

526 While the outcome of infection with *M. tuberculosis* in humans is likely more a
527 spectrum than a bipolar, active vs. latent, state^{64,65}, infection with *M. tuberculosis* in cattle
528 could be indicative of a latent infection being established, as compared to an active disease
529 status upon *M. bovis* infection. The bovine infection model may therefore offer a tractable
530 experimental system in which to explore the reactivation of *M. tuberculosis* infection and to
531 define prognostic biomarkers of the development of active disease. Furthermore, infection of
532 cattle with *M. tuberculosis* to establish latent infection may provide a tractable outbred model
533 in which to explore post-exposure vaccination strategies.

534

535 In conclusion, our work has shown that *M. tuberculosis* isolates, whether the H37Rv
536 type strain or a recent isolate, are attenuated for virulence in a bovine infection model as
537 compared to *M. bovis*. This work provides further evidence of the distinct host preference of
538 tubercle bacilli as a basis to explore the molecular basis of virulence in *M. bovis* as compared
539 to *M. tuberculosis*, and also offers a model in which to explore the reactivation of latent TB
540 infection.

541

542

543

544

545 **Funding Sources**

546 We gratefully acknowledge funding from: the European Commission's Seventh Framework
547 Programme (FP7, 2007-2013) Research Infrastructures Action under the grant agreement No.
548 FP7-228394 (NADIR project); EC H2020 program grant number 643381 (TBVAC2020);
549 Wellcome Trust grant number 075833/A/04/Z under their "Animal health in the developing
550 world" initiative; Wellcome Trust PhD awards 097429/Z/11/Z (K.R-A.) and 102395/Z/13/Z
551 (A.S.); Science Foundation Ireland Investigator Award 08/IN.1/B2038 (SG).

552

553 **Acknowledgements**

554 The authors are grateful to the members of the scientific and animal staff of the Plate-Forme
555 d'Infectiologie Expérimentale, PFIE, INRA, 37380, Nouzilly, France, especially to the study
556 managers Céline Barc and Philippe Bernardet and animal technicians Olivier Boulesteix and
557 Joël Moreau.

References

- 1 WHO. http://www.who.int/tb/publications/global_report/en/, 2017).
- 2 Karlson, A. G. & Lessel, E. F. *Mycobacterium bovis* nom. nov. *Int J Syst Bacteriol* **20**, 273-282 (1970).
- 3 Wells, A. G. The murine type of tubercle bacillus (The vole acid-fast bacillus). *MRC Spec. Rep. Ser. med. Res. Coun., Lond.* (1946).
- 4 Cousins, D. V., Peet, R. L., Gaynor, W. T., Williams, S. N. & Gow, B. L. Tuberculosis in imported hyrax (*Procavia capensis*) caused by an unusual variant belonging to the *Mycobacterium tuberculosis* complex. *Veterinary microbiology* **42**, 135-145 (1994).
- 5 Smith, N. The 'Dassie' bacillus. *Tubercle* **41**, 203-212 (1960).
- 6 Aranaz, A. *et al.* *Mycobacterium tuberculosis* subsp. *caprae* subsp. nov.: a taxonomic study of a new member of the *Mycobacterium tuberculosis* complex isolated from goats in Spain. *Int J Syst Bacteriol* **49 Pt 3**, 1263-1273 (1999).
- 7 Cousins, D. V. *et al.* Tuberculosis in seals caused by a novel member of the *Mycobacterium tuberculosis* complex: *Mycobacterium pinnipedii* sp. nov. *International journal of systematic and evolutionary microbiology* **53**, 1305-1314 (2003).
- 8 van Ingen, J. *et al.* Characterization of *Mycobacterium orygis* as *M. tuberculosis* complex subspecies. *Emerging infectious diseases* **18**, 653-655, doi:10.3201/eid1804.110888 (2012).
- 9 Alexander, K. A. *et al.* Novel *Mycobacterium tuberculosis* complex pathogen, *M. mungi*. *Emerging infectious diseases* **16**, 1296-1299, doi:10.3201/eid1608.100314 (2010).
- 10 Francis, J. Control of infection with the bovine tubercle bacillus. *Lancet* **1**, 34-39 (1950).
- 11 Magnus, K. Epidemiological Basis of Tuberculosis Eradication 3. Risk of Pulmonary Tuberculosis after Human and Bovine Infection. *Bull World Health Organ.* **35**, 483-508 (1966).
- 12 Koch, R. An Address on the Fight against Tuberculosis in the Light of the Experience that has been Gained in the Successful Combat of other Infectious Diseases. *Br Med J* **2**, 189-193 (1901).
- 13 Whelan, A. O. *et al.* Revisiting Host Preference in the *Mycobacterium tuberculosis* Complex: Experimental Infection Shows *M. tuberculosis* H37Rv to Be Avirulent in Cattle. *Plos One* **5**, doi:10.1371/journal.pone.0008527 (2010).
- 14 von Berhing, E. in *Nobel Lectures, Physiology or Medicine 1901-1921* (Elsevier Publishing Company, 1901).
- 15 Cole, S. T. *et al.* Deciphering the biology of *Mycobacterium tuberculosis* from the complete genome sequence. *Nature* **393**, 537-544, doi:10.1038/31159 (1998).
- 16 Garnier, T. *et al.* The complete genome sequence of *Mycobacterium bovis*. *Proc Natl Acad Sci U S A* **100**, 7877-7882, doi:10.1073/pnas.1130426100 (2003).
- 17 Malone, K. M. *et al.* Updated Reference Genome Sequence and Annotation of *Mycobacterium bovis* AF2122/97. *Genome Announc* **5**, doi:10.1128/genomeA.00157-17 (2017).
- 18 Groschel, M. I., Sayes, F., Simeone, R., Majlessi, L. & Brosch, R. ESX secretion systems: mycobacterial evolution to counter host immunity. *Nat Rev Microbiol* **14**, 677-691, doi:10.1038/nrmicro.2016.131 (2016).
- 19 Brodin, P. *et al.* Bacterial artificial chromosome-based comparative genomic analysis identifies *Mycobacterium microti* as a natural ESAT-6 deletion mutant. *Infect Immun* **70**, 5568-5578 (2002).
- 20 Mostowy, S., Cousins, D. & Behr, M. A. Genomic interrogation of the dassie bacillus reveals it as a unique RD1 mutant within the *Mycobacterium tuberculosis* complex. *J Bacteriol* **186**, 104-109 (2004).
- 21 Gonzalo-Asensio, J. *et al.* Evolutionary history of tuberculosis shaped by conserved mutations in the PhoPR virulence regulator. *Proc Natl Acad Sci U S A* **111**, 11491-11496, doi:10.1073/pnas.1406693111 (2014).
- 22 Behr, M. A. & Gordon, S. V. Why doesn't *Mycobacterium tuberculosis* spread in animals? *Trends Microbiol* **23**, 1-2, doi:10.1016/j.tim.2014.11.001 (2015).

23 Steenken, W., Oatway, W. H. & Petroff, S. A. Biological Studies of the Tubercl Bacillus :
Iii. Dissociation and Pathogenicity of the R and S Variants of the Human Tubercl Bacillus
(H(37)). *J Exp Med* **60**, 515-540 (1934).

24 Ioerger, T. R. *et al.* Variation among genome sequences of H37Rv strains of *Mycobacterium*
tuberculosis from multiple laboratories. *J Bacteriol* **192**, 3645-3653, doi:10.1128/JB.00166-
10 (2010).

25 Cadmus, S. *et al.* Molecular analysis of human and bovine tubercle bacilli from a local
setting in Nigeria. *J Clin Microbiol* **44**, 29-34, doi:10.1128/JCM.44.1.29-34.2006 (2006).

26 Chen, Y. *et al.* Potential challenges to the Stop TB Plan for humans in China; cattle maintain
M. bovis and *M. tuberculosis*. *Tuberculosis (Edinb)* **89**, 95-100,
doi:10.1016/j.tube.2008.07.003 (2009).

27 Ocepek, M., Pate, M., Zolnir-Dovc, M. & Poljak, M. Transmission of *Mycobacterium*
tuberculosis from human to cattle. *J Clin Microbiol* **43**, 3555-3557,
doi:10.1128/JCM.43.7.3555-3557.2005 (2005).

28 Ameni, G. *et al.* *Mycobacterium tuberculosis* infection in grazing cattle in central Ethiopia.
Vet J **188**, 359-361, doi:10.1016/j.tvjl.2010.05.005 (2011).

29 Berg, S. *et al.* The burden of mycobacterial disease in ethiopian cattle: implications for
public health. *PLoS One* **4**, e5068, doi:10.1371/journal.pone.0005068 (2009).

30 Firdessa, R. *et al.* Mycobacterial lineages causing pulmonary and extrapulmonary
tuberculosis, Ethiopia. *Emerging infectious diseases* **19**, 460-463,
doi:10.3201/eid1903.120256 (2013).

31 Comas, I., Homolka, S., Niemann, S. & Gagneux, S. Genotyping of genetically
monomorphic bacteria: DNA sequencing in *Mycobacterium tuberculosis* highlights the
limitations of current methodologies. *PLoS One* **4**, e7815, doi:10.1371/journal.pone.0007815
(2009).

32 Stucki, D. *et al.* *Mycobacterium tuberculosis* lineage 4 comprises globally distributed and
geographically restricted sublineages. *Nat Genet* **48**, 1535-1543, doi:10.1038/ng.3704
(2016).

33 Gallagher, J. & Horwill, D. M. A selective oleic acid albumin agar medium for the
cultivation of *Mycobacterium bovis*. *J Hyg (Lond)* **79**, 155-160 (1977).

34 Gordon, S. V. *et al.* Identification of variable regions in the genomes of tubercle bacilli using
bacterial artificial chromosome arrays. *Mol Microbiol* **32**, 643-655 (1999).

35 Kamerbeek, J. *et al.* Simultaneous detection and strain differentiation of *Mycobacterium*
tuberculosis for diagnosis and epidemiology. *J Clin Microbiol* **35**, 907-914 (1997).

36 Whelan, A. *et al.* Immunogenicity comparison of the intradermal or endobronchial boosting
of BCG vaccines with Ad5-85A. *Vaccine* **30**, 6294-6300,
doi:10.1016/j.vaccine.2012.07.086 (2012).

37 Vordermeier, H. M. *et al.* Correlation of ESAT-6-specific gamma interferon production with
pathology in cattle following *Mycobacterium bovis* BCG vaccination against experimental
bovine tuberculosis. *Infect Immun* **70**, 3026-3032 (2002).

38 Vordermeier, H. M. *et al.* Viral booster vaccines improve *Mycobacterium bovis* BCG-
induced protection against bovine tuberculosis. *Infect Immun* **77**, 3364-3373,
doi:10.1128/IAI.00287-09 (2009).

39 Wangoo, A. *et al.* Advanced granulomatous lesions in *Mycobacterium bovis*-infected cattle
are associated with increased expression of type I procollagen, gammadelta (WC1+) T cells
and CD 68+ cells. *J Comp Pathol* **133**, 223-234, doi:10.1016/j.jcpa.2005.05.001 (2005).

40 Martin, M. Cutadapt Removes Adapter Sequences From High-Throughput Sequencing
Reads. *EMBnet.journal* (2011).
[<http://journal.embnet.org/index.php/embnetjournal/article/view/200>](http://journal.embnet.org/index.php/embnetjournal/article/view/200).

41 Bushnell, B. *BBMap* short read aligner, and other bioinformatic tools,
<sourceforge.net/projects/bbmap/> (2017).

42 Andrew, S. *FastQC*,
<<http://www.bioinformatics.babraham.ac.uk/projects/fastqc/>> (2017).

43 Dobin, A. *et al.* STAR: ultrafast universal RNA-seq aligner. *Bioinformatics* **29**, 15-21, doi:10.1093/bioinformatics/bts635 (2013).

44 Liao, Y., Smyth, G. K. & Shi, W. featureCounts: an efficient general purpose program for assigning sequence reads to genomic features. *Bioinformatics* **30**, 923-930, doi:10.1093/bioinformatics/btt656 (2014).

45 Robinson, M. D., McCarthy, D. J. & Smyth, G. K. edgeR: a Bioconductor package for differential expression analysis of digital gene expression data. *Bioinformatics* **26**, 139-140, doi:10.1093/bioinformatics/btp616 (2010).

46 Foroushani, A. B., Brinkman, F. S. & Lynn, D. J. Pathway-GPS and SIGORA: identifying relevant pathways based on the over-representation of their gene-pair signatures. *PeerJ* **1**, e229, doi:10.7717/peerj.229 (2013).

47 Wickham, H. *ggplot2: Elegant Graphics for Data Analysis*. (Springer-Verlag, 2009).

48 Chen, H. *VennDiagram: Generate High-Resolution Venn and Euler Plots*, <<https://cran.r-project.org/web/packages/VennDiagram/index.html>> (2016).

49 Golby, P., Villarreal-Ramos, B., Dean, G., Jones, G. J. & Vordermeier, M. MicroRNA expression profiling of PPD-B stimulated PBMC from *M. bovis*-challenged unvaccinated and BCG vaccinated cattle. *Vaccine* **32**, 5839-5844, doi:10.1016/j.vaccine.2014.07.034 (2014).

50 Aranday-Cortes, E. *et al.* Upregulation of IL-17A, CXCL9 and CXCL10 in early-stage granulomas induced by *Mycobacterium bovis* in cattle. *Transbound Emerg Dis* **60**, 525-537, doi:10.1111/j.1865-1682.2012.01370.x (2013).

51 Castel, S. E., Levy-Moonshine, A., Mohammadi, P., Banks, E. & Lappalainen, T. Tools and best practices for data processing in allelic expression analysis. *Genome Biol* **16**, 195, doi:10.1186/s13059-015-0762-6 (2015).

52 Tarazona, S., Garcia-Alcalde, F., Dopazo, J., Ferrer, A. & Conesa, A. Differential expression in RNA-seq: a matter of depth. *Genome Res* **21**, 2213-2223, doi:10.1101/gr.124321.111 (2011).

53 Wang, Y. *et al.* Evaluation of the coverage and depth of transcriptome by RNA-Seq in chickens. *BMC Bioinformatics* **12 Suppl 10**, S5, doi:10.1186/1471-2105-12-S10-S5 (2011).

54 O'Neill, A. S., van den Berg, T. K. & Mullen, G. E. Sialoadhesin - a macrophage-restricted marker of immunoregulation and inflammation. *Immunology* **138**, 198-207, doi:10.1111/imm.12042 (2013).

55 Hall, J. D. *et al.* The impact of chemokine receptor CX3CR1 deficiency during respiratory infections with *Mycobacterium tuberculosis* or *Francisella tularensis*. *Clin Exp Immunol* **156**, 278-284, doi:10.1111/j.1365-2249.2009.03882.x (2009).

56 Sakai, S. *et al.* Cutting edge: control of *Mycobacterium tuberculosis* infection by a subset of lung parenchyma-homing CD4 T cells. *J Immunol* **192**, 2965-2969, doi:10.4049/jimmunol.1400019 (2014).

57 Aranday-Cortes, E. *et al.* Transcriptional profiling of disease-induced host responses in bovine tuberculosis and the identification of potential diagnostic biomarkers. *PLoS One* **7**, e30626, doi:10.1371/journal.pone.0030626 (2012).

58 Yu, C. H. *et al.* RP105 Engages Phosphatidylinositol 3-Kinase p110delta To Facilitate the Trafficking and Secretion of Cytokines in Macrophages during Mycobacterial Infection. *J Immunol* **195**, 3890-3900, doi:10.4049/jimmunol.1500017 (2015).

59 Feng, Y. *et al.* Platelets direct monocyte differentiation into epithelioid-like multinucleated giant foam cells with suppressive capacity upon mycobacterial stimulation. *J Infect Dis* **210**, 1700-1710, doi:10.1093/infdis/jiu355 (2014).

60 Sallin, M. A. *et al.* Th1 Differentiation Drives the Accumulation of Intravascular, Non-protective CD4 T Cells during Tuberculosis. *Cell Rep* **18**, 3091-3104, doi:10.1016/j.celrep.2017.03.007 (2017).

61 Salgame, P. MMPs in tuberculosis: granuloma creators and tissue destroyers. *J Clin Invest* **121**, 1686-1688, doi:10.1172/JCI57423 (2011).

62 Sathyamoorthy, T. *et al.* Membrane Type 1 Matrix Metalloproteinase Regulates Monocyte
Migration and Collagen Destruction in Tuberculosis. *J Immunol* **195**, 882-891,
doi:10.4049/jimmunol.1403110 (2015).

63 Koguchi, Y. *et al.* High plasma osteopontin level and its relationship with interleukin-12-
mediated type 1 T helper cell response in tuberculosis. *Am J Respir Crit Care Med* **167**,
1355-1359, doi:10.1164/rccm.200209-1113OC (2003).

64 Barry, C. E., 3rd *et al.* The spectrum of latent tuberculosis: rethinking the biology and
intervention strategies. *Nat Rev Microbiol* **7**, 845-855, doi:10.1038/nrmicro2236 (2009).

65 Esmail, H. *et al.* Characterization of progressive HIV-associated tuberculosis using 2-deoxy-
2-[18F]fluoro-D-glucose positron emission and computed tomography. *Nat Med* **22**, 1090-
1093, doi:10.1038/nm.4161 (2016).

Table 1: Bacteriology of investigated organs.

| Strain | <i>M. bovis</i> AF2122/97 | | | | <i>M. tuberculosis</i> H37Rv | | | | <i>M. tuberculosis</i> BTB1558 | | | |
|----------------------|---------------------------|------|------|------|------------------------------|------|------|------|--------------------------------|------|------|------|
| Animal ID | 1217 | 1221 | 1222 | 1224 | 1201 | 1203 | 1213 | 1211 | 1202 | 1207 | 1209 | 1215 |
| Head LN [¶] | 0/8 * | 2/8 | 6/8 | 5/8 | 0/8 | 1/8 | 2/6 | 0/8 | 2/7 | 2/8 | 1/8 | 1/8 |
| Resp LN [¶] | 5/5 | 5/5 | 4/5 | 5/5 | 1/5 | 2/5 | 2/5 | 3/5 | 3/5 | 1/5 | 4/4 | 2/5 |
| Lung* | 2/2 | 1/2 | 1/1 | 2/2 | 0/1 | 0/1 | 0/1 | 0/1 | 0/1 | 0/1 | 0/1 | 0/1 |

[¶]LN = lymph nodes; see Materials and Methods for details of tissues examined.

*Number of tissues sampled in each organ system per challenged animal that were confirmed as culture positive with the respective infecting strain; hence 0/8 in head lymph nodes means no positive cultures from 8 samples taken.

Table 2: Granuloma presentations in infected cattle

| Strain | Stage I[¶] | Stage II | Stage III | Stage IV |
|------------------------------|----------------------------|-----------------|------------------|-----------------|
| <i>M. tuberculosis</i> H37Rv | 31 | 2 | 0 | 0 |
| <i>M. tuberculosis</i> H37Rv | 20 | 5 | 0 | 0 |
| <i>M. bovis</i> AF2122/97 | 74 | 117 | 51 | 81 |

[¶]Sections were scored for granuloma stages: stage I (initial), stage II (solid), stage III (necrotic) and stage IV (mineralised). Granuloma development in both *M. tuberculosis* strains is significantly different from *M. bovis* AF2122/97, $P<0.001$ (X-sq for trend)

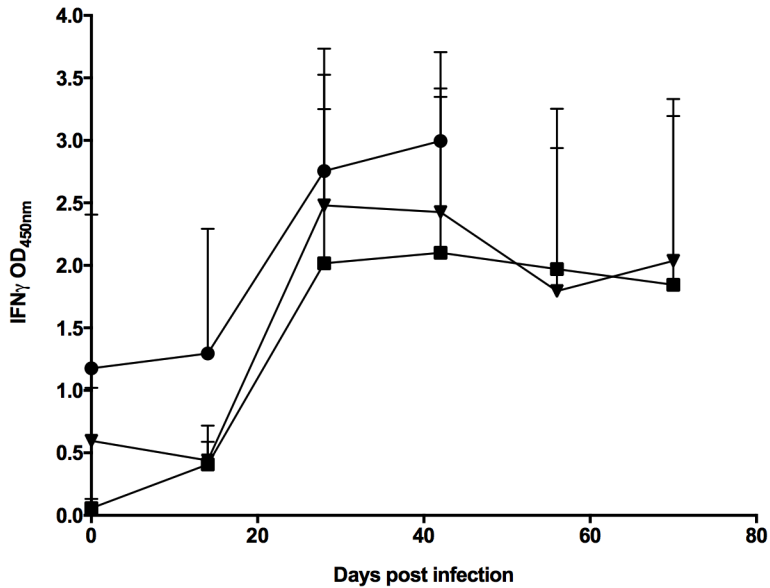


Figure 1: Infection of cattle with *M. tuberculosis* H37Rv, *M. tuberculosis* BTB1558 or *M. bovis* AF2122/97 induces similar peripheral immune responses.

Blood was collected at regular intervals from cattle prior to and after experimental infection with *M. tuberculosis* H37Rv (n=4), *M. tuberculosis* BTB1558 (n=4), or *M. bovis* AF2122/97 (n=4). Whole blood was isolated and stimulated with a cocktail of peptides derived from ESAT-6 and CFP-10. The responses in the infected cattle are shown: *M. tuberculosis* H37Rv (squares); *M. tuberculosis* BTB1558 (triangles); *M. bovis* AF2122/97 (circles). *M. bovis* infected animals were maintained for 6 weeks, *M. tuberculosis* groups for 10 weeks. Data for each time point is presented as the mean response \pm SEM.

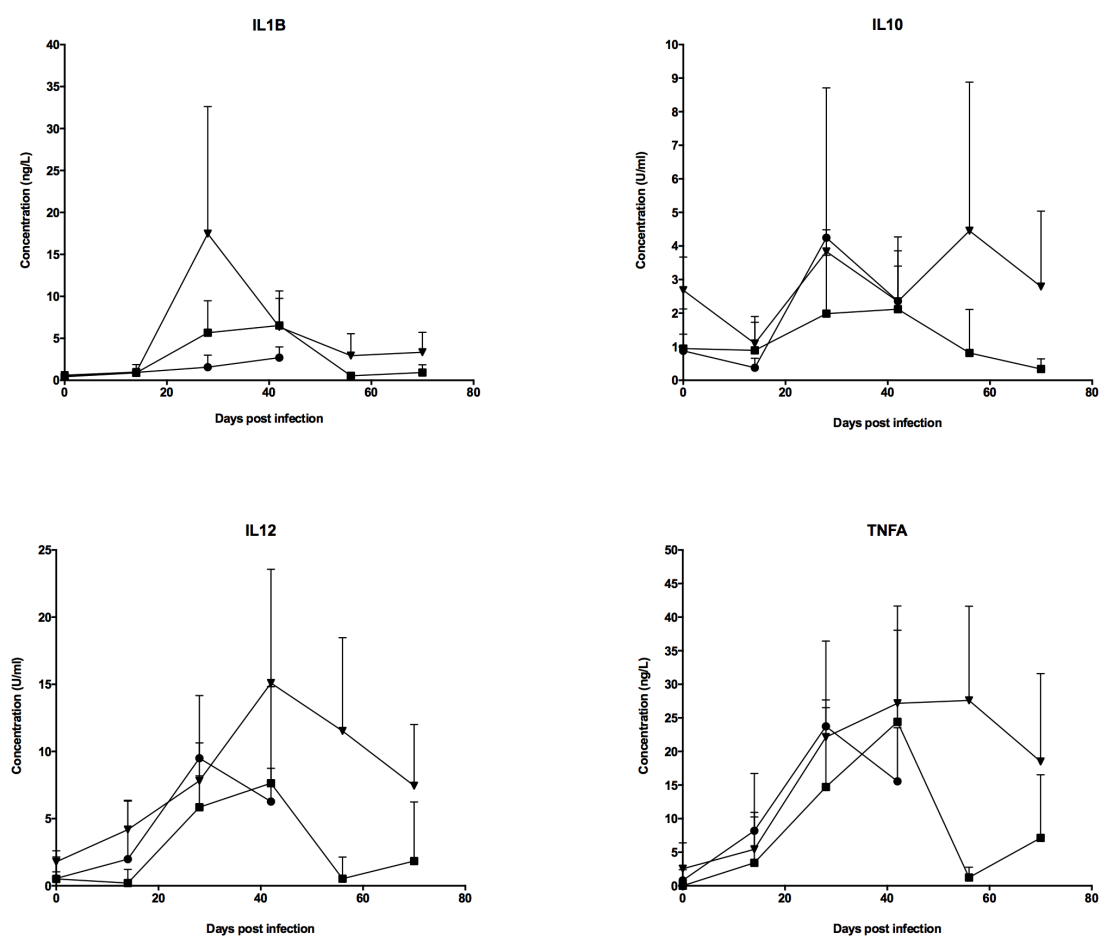


Figure 2: Cytokine analysis of stimulated whole blood from *M. tuberculosis* H37Rv, *M. tuberculosis* BTB1558 or *M. bovis* AF2122/97 infected cattle

PPD-B stimulated-whole blood supernatants were assayed for IL-1 β , IL-10, IL-12 (D), and TNF- α cytokine levels using a custom-designed bovine MSD. The response in the *M. tuberculosis* H37Rv infected cattle is shown as squares; *M. tuberculosis* BTB1558 is shown as triangles; and *M. bovis* AF2122/97 shown as circles; all groups contained 4 animals. IL-10 and IL-12 responses are reported as U/ml while IL-1 β and TNF- α responses are reported in ng/ml as interpolated from the standard curves for each cytokine included on each plate. Data for each time point is presented as the mean response \pm SEM.

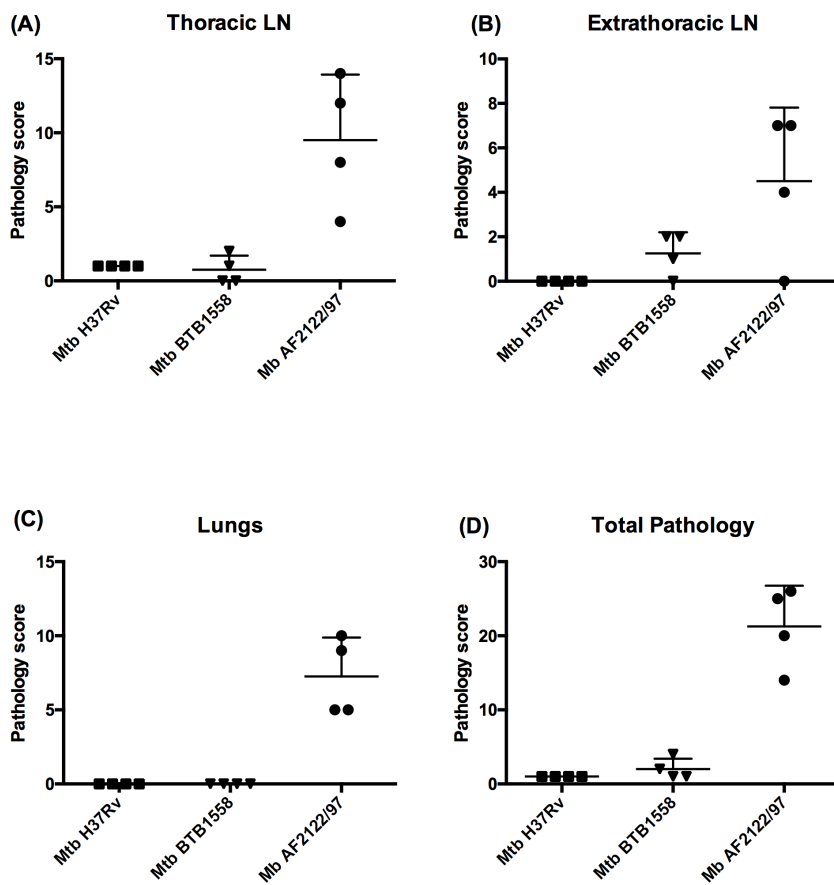


Figure 3: Pathology scores across *M. tuberculosis* H37Rv, *M. tuberculosis* BTB1558 or *M. bovis* AF2122/97 infected cattle

Pathology scores in the thoracic (A), extra thoracic lymph nodes (LN) (B), and lungs (C) of animals infected with *M. tuberculosis* H37Rv (squares); *M. tuberculosis* BTB1558 (triangles), or *M. bovis* AF2122/97 (circles). Total gross pathology score is shown in (D). Data for each time point is presented as the mean response \pm SEM. This difference was statistically significant in the lungs (p 0.0052) and in the total pathology score (p 0.0105).

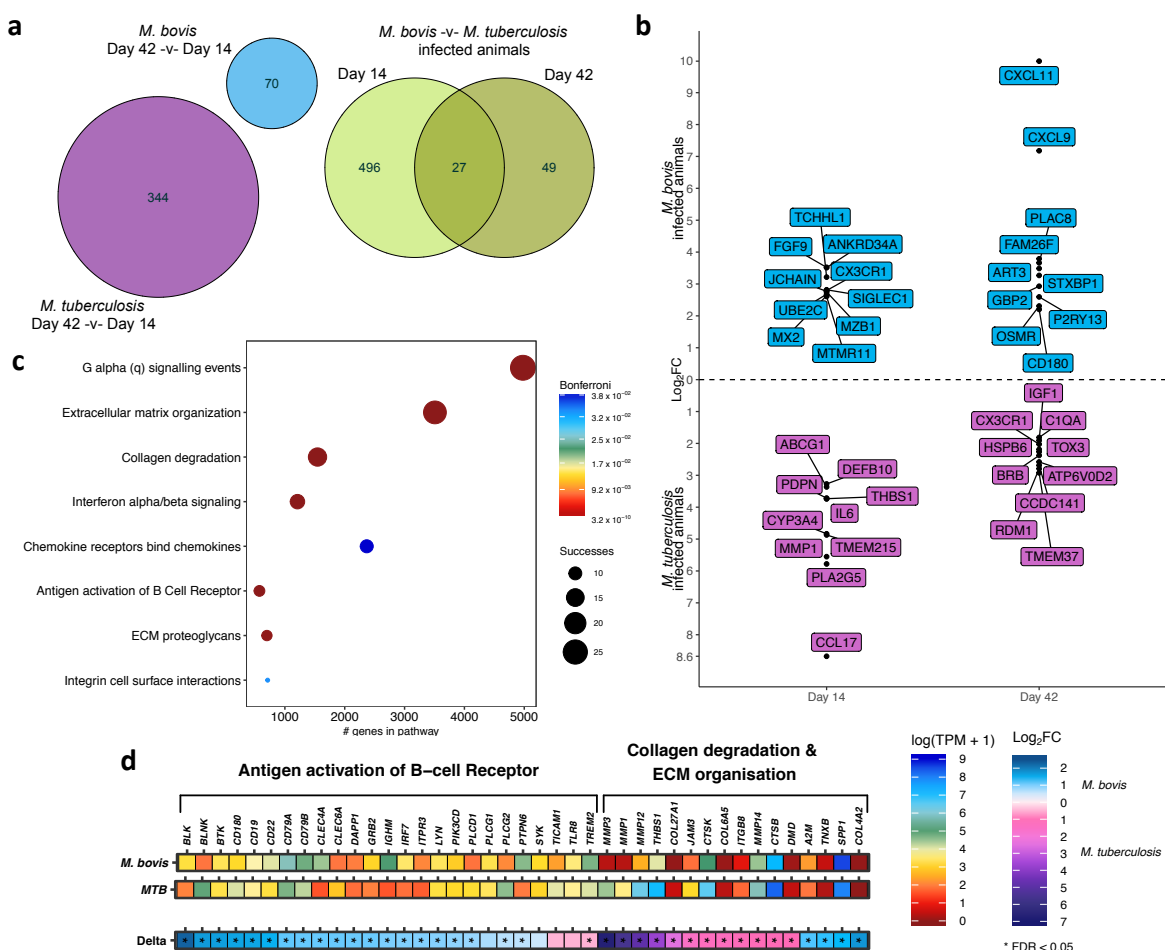


Figure 4: Transcriptome analysis of unstimulated whole blood after *M. bovis* AF2122/97 or *M. tuberculosis* H37Rv infection

(A) The number of differentially expressed genes in unstimulated whole blood for *M. bovis*- (blue) and *M. tuberculosis*- (purple) infected animals at day 42 -v- day 14 post infection ($-1 > \log_2\text{FC} < 1$, FDR < 0.05). The green Venn diagram depicts the overlap of differentially expressed genes from the direct comparison of unstimulated whole blood samples from *M. bovis* and *M. tuberculosis* infected animals at day 14 and day 42 post infection ($-1 > \log_2\text{FC} < 1$, FDR < 0.05). (B) The top 10 differentially expressed genes between *M. bovis*- (blue) and *M. tuberculosis*- (purple) infected animals at day 14- and day 42-post infection (FDR < 0.05). The graph depicts positive relative log₂ fold change values where a gene that shows increased expression in *M. bovis* infected animals is relative to its expression in *M. tuberculosis* infected animals and vice versa. (C) Pathway enrichment analysis results for the list of 523 differentially expressed genes between *M. bovis* and *M. tuberculosis* infected animals at day 14-post infection. The graph depicts the enrichment of each pathway in the differentially expressed gene list based on the SIGORA successes metric (circle size) and the number of genes annotated within the pathway (“#genes in pathway”) while the colour bar depicts the significance of the association (Bonferroni < 0.05). (D) The relative expression (transcripts per million, TPM, “log(TPM + 1)”) and the relative change in expression (log₂ fold

change (“Log₂FC”)) of the genes belonging to the Antigen activation of B cell Receptor (R-HSA-983695), Collagen degradation (R-HSA-1442490) and Extracellular matrix (“ECM”) organization (R-HSA-1474244) pathways enriched for the comparison of *M. bovis* and *M. tuberculosis* infected animals at day 14 post infection. Genes that pass multiple hypothesis testing are denoted with an asterisk (Benjamini-Hochberg, FDR < 0.05) (*).

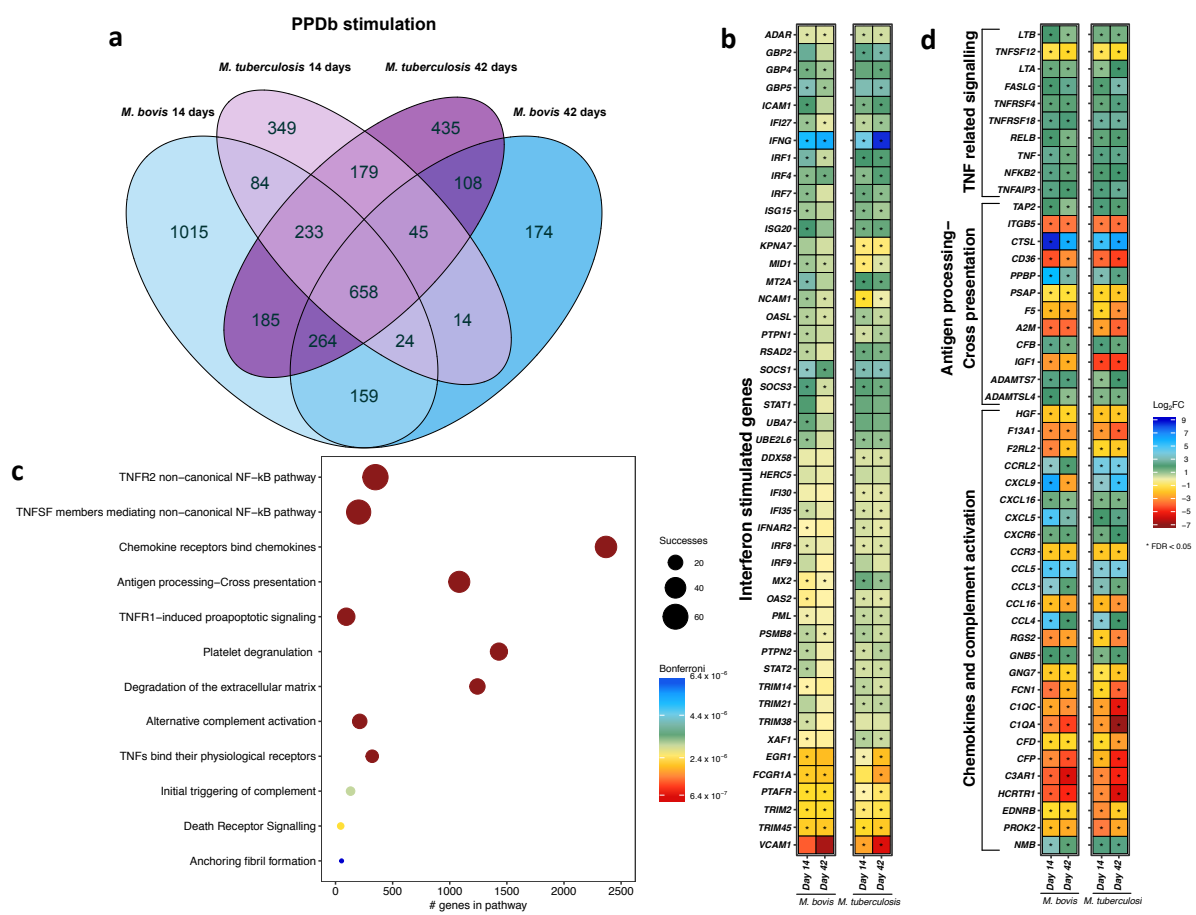


Figure 5: Comparative transcriptome analysis of unstimulated vs. PPD-B stimulated whole blood from *M. bovis* AF2122/97 or *M. tuberculosis* H37Rv infected cattle

(A) The overlap of differentially expressed genes from the comparison of unstimulated whole blood samples and PPD-B stimulated whole blood samples for *M. bovis* AF2122/97 infected animals at day 14 and day 42 (blue) and *M. tuberculosis* H37Rv infected animals at day 14 and day 42 (purple) ($-1 > \log_2 FC < 1$, FDR < 0.05). (B) The relative expression of Interferon stimulated genes (R-HSA-877300) from the comparison of unstimulated whole blood samples and PPD-B stimulated whole blood samples for *M. bovis* AF2122/97 infected animals at day 14 and day 42 (blue) and *M. tuberculosis* H37Rv infected animals at day 14 and day 42 (purple). Genes that pass multiple hypothesis testing are denoted with an asterisk (Benjamini-Hochberg, FDR < 0.05) (*). (C) Pathway enrichment analysis results for 658 genes that are significantly differentially expressed ($-1 > \log_2 FC < 1$, FDR < 0.05) in PPD-B stimulated whole blood samples from both *M. bovis* AF2122/97- and *M. tuberculosis* H37Rv- infected animals at both 14 and 42 days post infection in comparison to unstimulated whole blood samples. The graph depicts the association of each pathway with the differentially expressed gene list based on the SIGORA successes metric (circle size) and the number of genes annotated within the pathway ("#genes in pathway") while the colour bar depicts the significance of the association (Bonferroni < 0.05). (D) The relative expression (transcripts per million, TPM, "log(TPM +1)") and the relative change in expression (\log_2 fold change ("Log₂FC"))

of 658 genes that are significantly differentially expressed ($-1 > \log_2\text{FC} < 1$, $\text{FDR} < 0.05$) in PPD-B stimulated whole blood samples from both *M. bovis* AF2122/97- and *M. tuberculosis* H37Rv-infected animals at both 14 and 42 days post infection in comparison to unstimulated whole blood samples. The genes are associated with pathways related to TNF signalling (R-HSA-5668541, R-HSA-5676594, R-HSA-5357786, R-HSA-5669034), Antigen processing-Cross presentation (R-HSA-1236975) and Chemokines and complement activation (R-HSA-380108, R-HSA-173736). Genes that pass multiple hypothesis testing are denoted with an asterisk (Benjamini-Hochberg, $\text{FDR} < 0.05$) (*).

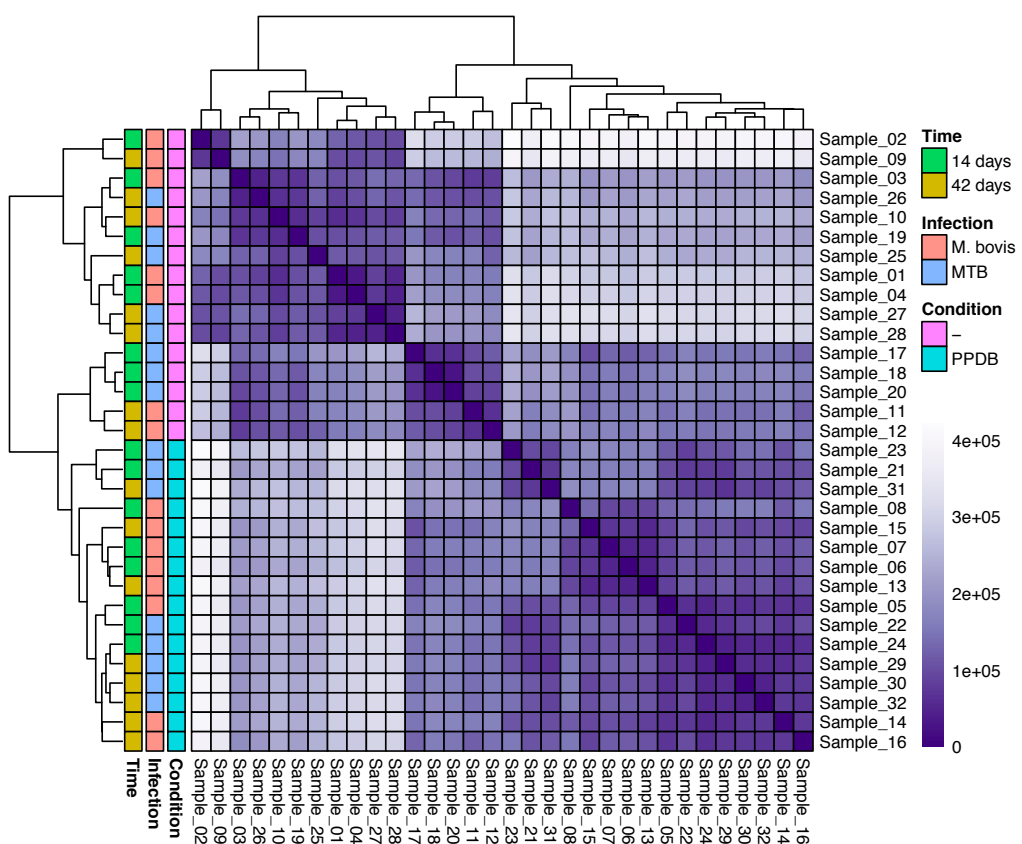


Figure S1: Genome-wide gene expression correlation

Genome-wide gene expression correlation between the 32 study samples pertaining to whole blood samples (unstimulated (“-”) or PPDB-stimulated (“PPDB”)) from cattle infected with either *M. bovis* AF2122/97 (“*M. bovis*”) or *M. tuberculosis* H37Rv (“MTB”) 14 days or 42 days (“Time”) post infection. Samples are clustered using Euclidean distance and coloured bars on the left of the plot denote the variables time point (“Time”), infection status (“Infection”) and stimulation status (“Condition”) for each of the 32 samples.

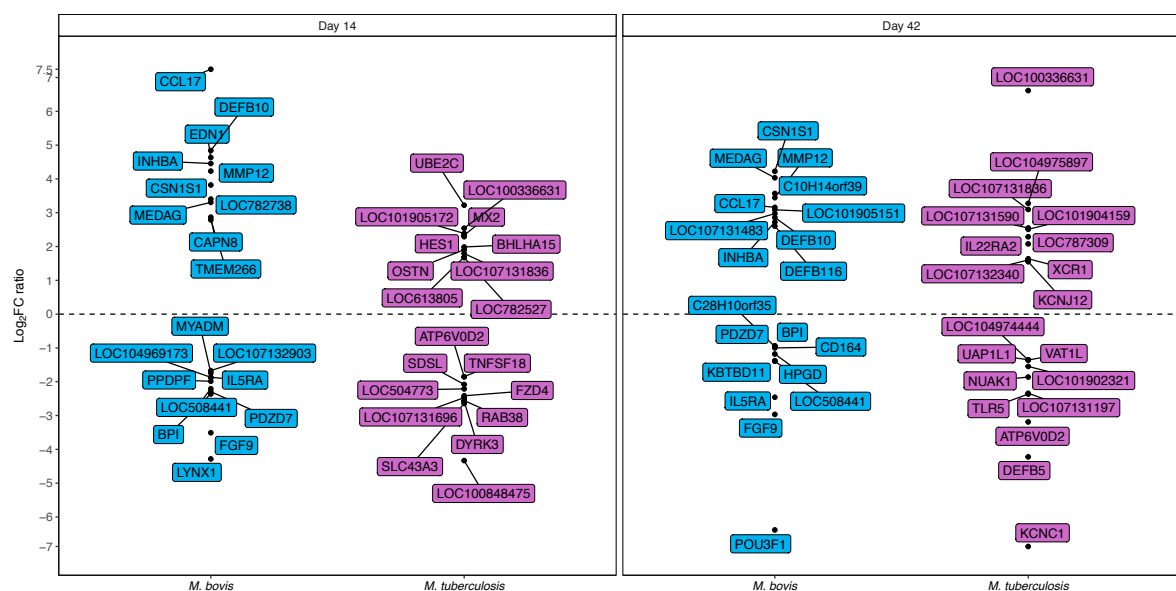


Figure S2: Top DE genes in unstimulated vs. stimulated whole blood between *M. bovis* AF2122/97 and *M. tuberculosis* H37Rv infected animals

The top 10 upregulated and top 10 downregulated differentially expressed genes in whole blood samples derived from *M. bovis* AF2122/97 versus *M. tuberculosis* H37Rv infected animals and stimulated with PPD-B at day 14 and day 42 post infection. The change in gene expression from the comparison of stimulated blood to unstimulated blood at each time point for either *M. bovis* AF2122/97 or *M. tuberculosis* H37Rv infected animals was used to calculate log₂FC ratio (i.e. expression of gene X in *M. bovis* AF2122/97 infected animals at day 14-post infection divided by expression of gene X in *M. tuberculosis* H37Rv infected animals at day 14-post infection).

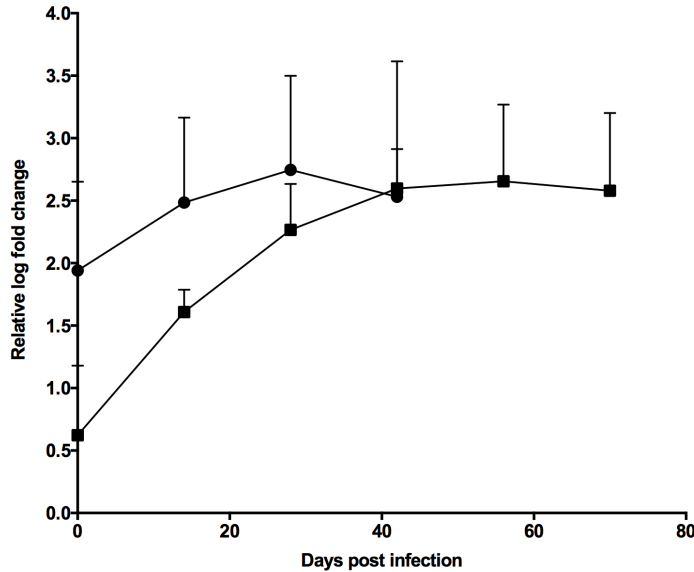


Figure S3: miR-155 analysis across *M. bovis* AF2122/97 and *M. tuberculosis* H37Rv infected animals

The level of miR-155 in PPD-B stimulated vs. unstimulated whole blood from *M. bovis* AF2122/97 (circles) and *M. tuberculosis* H37Rv (squares) infected cattle was assessed over the infection time course using RT-qPCR with Exiqon miRCURY UniRT miRNA hsa-miR-155-5p primers.